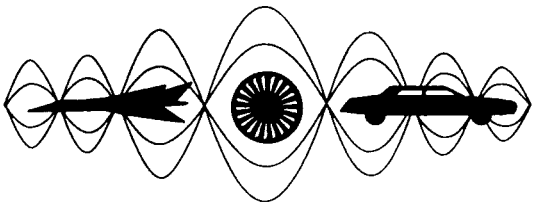

FIFTH INTERNATIONAL CONGRESS ON SOUND AND VIBRATION
DECEMBER 15-18, 1997
ADELAIDE, SOUTH AUSTRALIA

MECHANICAL SIGNATURE ENHANCEMENT OF RESPONSE VIBRATIONS IN THE TIME LAG DOMAIN

By
Y. Gao, R. Ford and R.B. Randall
School of Mechanical and Manufacturing Engineering
University of New South Wales
Sydney 2052

ABSTRACT

Signature analysis deals with the extraction of information from measured signal patterns and this paper proposes a new procedure to enhance the mechanical signature related to a faulty element in a rotating machine. The enhancement operation is implemented in the time lag domain using envelope signals which are obtained using a multiple carrier amplitude demodulation technique. This procedure is studied theoretically. Also it is evaluated using simulated digital sequences and vibration measurements from a railway track and a paper machine.

1. INTRODUCTION

In vibration analysis, mechanical signatures can be considered to be measured response vibration patterns which characterise a specific vibration source and convey information about it [1]. Mechanical faults in rotating machines often generate a sequence of impulses with a given repetition rate. Each of such impulses excites resonances of the system under measurement and the resonant vibrations usually die out very quickly because of energy dissipation in the system. Consequently, the response vibrations caused by such impulsive sources show up as a sequence of damped impulse responses which have the same repetition rate as the impulse sequence generated by the mechanical faults. This mechanical signature can be interpreted as amplitude modulation and has been widely used to diagnose mechanical faults in rotating machines [2, 3].

Bandpass Filtered Envelope Analysis, in brief BFEA, (bandpass filtering and amplitude demodulation) [2, 4] is one of the techniques used to diagnose mechanical faults in rotating machines by analysing the signature mentioned above. Optimum application of this technique depends upon the choice of a proper frequency band, in which the vibration is mainly caused by the mechanical faults in question. In practice, this frequency band can be chosen by comparing spectra measured at different stages of deterioration and inspecting the variation of vibration levels in different frequency bands. A measurement at an initial stage is very useful

for this purpose, but in the case where an initial measurement is not available, different frequency bands have to be tried experimentally.

In Reference [3], a multiple carrier amplitude demodulation procedure (MCAD) was proposed, which is non-band-dependent and has been found very useful in many practical applications because of its simple implementation and more valid trending indication. In the case of a low Signal-to-Noise Ratio (SNR), however, the MCAD procedure might not be able to reveal the signature of a mechanical fault because of noise masking effects.

In this paper, a new procedure based on the MCAD procedure is designed to enhance the signature of a mechanical fault in rotating machines.

2. MULTIPLE CARRIER AMPLITUDE DEMODULATION

Usually, incipient mechanical faults in rotating machines can excite more than one resonance of a system in a very wide frequency band. These resonances are all modulated in a very similar way and can be approximated as [3]:

$$x_1(t) = M(t)\sum_{i=1}^{N} A_i e^{j\alpha_i} \tag{2.1}$$

where $\alpha_i = \omega_i t + \varphi_i$ and $M(t)$ is a real and positive function representing the envelope of mechanical fault signals. It includes the periodic exponential decays associated with each resonance which for simplicity are thus assumed to have approximately the same time constant (the actual envelope would be dominated by the longest time constant).

In practice, measured vibrations are usually contaminated by various types of background noise. These typically are band limited, and can be expressed as the sum of narrowband noise signals:

$$n(t) = N(t)\sum_{i=1}^{R} B_i e^{j\beta_i} \tag{2.2}$$

where $\beta = \omega_m t + \theta_i(t)$, $N(t)$ is a real and positive envelope function which varies slowly with time, $\theta_i(t)$ a slowly varying phase function, and ω_{ni} the central angular frequency of the ith narrowband noise component [5].

Mechanical faults in a rotating machine could also cause additive mechanical vibrations at the same time. Furthermore, even perfect mechanical elements in operation can contribute very strong, additive discrete frequency components, such as gear meshing frequencies. These additive frequency components can be expressed by their linear combination:

$$x_2(t) = \sum_{i=1}^{L} C_i e^{j\gamma_i} \tag{2.3}$$

where $\gamma_i = \Omega_i t + \Phi_i$.

Thus the measured response vibrations are usually the sum of Equations (2.1~3):

$$x(t) = M(t)\sum_{i=1}^{N} A_i e^{j\alpha_i} + N(t)\sum_{i=1}^{R} B_i e^{j\beta_i} + \sum_{i=1}^{L} C_i e^{j\gamma_i} \tag{2.4}$$

The modulus of the measured response vibrations can be expressed as:

$$|x(t)| = M_1(t)(1+y)^{\frac{1}{2}} \tag{2.5}$$

where: $$y=\frac{2}{M_1^2(t)}\Bigg[M^2(t)\sum_{i=1}^{N-1}\sum_{k=i+1}^{N}A_iA_k\cos(\alpha_i-\alpha_k)+N^2(t)\sum_{i=1}^{R-1}\sum_{k=i+1}^{R}B_iB_k\cos(\beta_i-\beta_k)+$$

$$+\sum_{i=1}^{L-1}\sum_{k=i+1}^{L}C_iC_k\cos(\gamma_i-\gamma_k)+M(t)N(t)\sum_{i=1}^{N}\sum_{k=1}^{R}A_iB_k\cos(\alpha_i-\beta_k)+ \quad (2.6a)$$

$$+M(t)\sum_{i=1}^{N}\sum_{k=1}^{L}A_iC_k\cos(\alpha_i-\gamma_k)+N(t)\sum_{i=1}^{L}\sum_{k=1}^{R}B_iC_k\cos(\beta_i-\gamma_k)\Bigg]-\frac{2P(t)}{M_1(t)}$$

$$M_1(t)=aM(t)+bN(t)+c \quad (2.6b)$$

$$P(t)=\frac{acM(t)+abM(t)N(t)+bcN(t)}{M_1(t)} \quad (2.6c)$$

and: $$a=\sqrt{\sum_{i=1}^{N}A_i^2};\ b=\sqrt{\sum_{i=1}^{R}B_i^2};\ c=\sqrt{\sum_{i=1}^{L}C_i^2}. \quad (2.6d)$$

It can be proved that [3]:

$$|y|\le 1 \quad (2.7)$$

Thus Equation (2.5) can be expanded into:

$$|x(t)|=M_1(t)\left(1+\frac{1}{2}y-\frac{1\cdot1}{2\cdot4}y^2+\frac{1\cdot1\cdot3}{2\cdot4\cdot6}y^3-\cdots\right) \quad (2.8)$$

By using the relationships in Equations (2.6a~d), Equation (2.8) can be rearranged as:

$$|x(t)|=f_1(t)+f_2(t) \quad (2.9)$$

where: $$f_1(t)=aM(t)+bN(t)+c-P(t) \quad (2.10)$$

and $$f_2(t)=M_1(t)\left[\frac{P(t)}{M_1(t)}+\frac{y}{2}-\frac{y^2}{8}+\frac{y^3}{16}-\cdots\right] \quad (2.11)$$

The above derivation shows that taking the modulus of response measurements demodulates the amplitude modulated vibrations. After this demodulation, the modulating function, $M(t)$, is enhanced by a factor, $a=\sqrt{\sum_{i=1}^{N}A_i^2}$, which reflects the power in all the carriers (thus the term Multiple Carrier Amplitude Demodulation, in brief MCAD). Also it is contaminated by $bN(t)$, $P(t)$ and $f_2(t)$.

The modulating function of interest is essentially a low frequency function. The contamination from $f_2(t)$ is essentially of high frequency components [3] which could be eliminated by lowpass filtration. Therefore, the main masking effects on $M(t)$ come from the second and fourth terms in Equation (2.10), both of which are of a random nature. How to reduce their masking effects on $M(t)$ to a certain extent and further enhance $M(t)$ will be discussed in the next section.

3. ENHANCMENT OF MECHANICAL FAULT SIGNATURES

Equation (2.9) shows that the MCAD technique can extract the modulating function, $M(t)$, contained in measured response vibrations. In many practical cases, the MCAD technique can clearly reveal the frequency components of the modulating function in the frequency domain [3].

However, the frequency components of the modulating function of $aM(t)$ might be masked in the case where the noise terms, $bN(t)$ and $P(t)$, in Equation (2.10) are high. $M(t)$ is a periodic function and correlates with itself in the whole time lag range. $N(t)$ and $P(t)$ are of random character. Both of them produce the highest correlation with themselves around zero

time lag and drop to very low levels away from zero time lag. Also the crosscovariance among the above three terms are at lower levels, compared with their autocovariances. These properties are very useful in suppressing the noise term to a considerable extent.

The autocovariance of $f_1(t)$ is:

$$C(\tau) = E[\{f_1(t) - u\}\{f_1(t+\tau) - u\}] = \lim_{T\to\infty} \frac{1}{T} \int_0^T \{f_1(t) - u\}\{f_1(t+\tau) - u\} dt \tag{3.1}$$

where:

$$\begin{aligned} u &= E[f_1(t)] \\ &= aE[M(t)] + bE[N(t)] + c + E[P(t)] \\ &= u_M + u_N + c + u_P \end{aligned} \tag{3.2}$$

Inserting Equation (2.10) into Equation (3.1) and using the relationships in Equation (3.2), we can produce:

$$C(\tau) = C_M(\tau) + C_N(\tau) + C_P(\tau) + C_{MNP}(\tau) \tag{3.3}$$

where:

$$\begin{aligned} C_M(\tau) &= E[\{aM(t) - u_M\}\{aM(t+\tau) - u_M\}] \\ C_N(\tau) &= E[\{bN(t) - u_N\}\{bN(t+\tau) - u_N\}] \\ C_P(\tau) &= E[\{P(t) - u_P\}\{P(t+\tau) - u_P\}] \end{aligned} \tag{3.4a}$$

and:

$$C_{MNP}(\tau) = C_{MN}(\tau) + C_{NM}(\tau) + C_{MP}(\tau) + C_{PM}(\tau) + C_{NP}(\tau) + C_{PN}(\tau) \tag{3.4b}$$

represent the corresponding auto- and crosscovariance functions, respectively. All the autocovariance functions are real even functions, while the crosscovariance functions are neither even nor odd functions, but they are related by:

$$C_{RS}(\tau) = C_{SR}(-\tau) \tag{3.5}$$

This relationship makes their sum a real even function, meaning that the autocovariance function, $C(\tau)$, in Equation (3.3) is a real even function and all its frequency components are cosine components.

Another useful property of autocovariance functions is:

$$C(0) = \sigma^2;\ C_M(0) = \sigma_M^2;\ C_N(0) = \sigma_N^2;\ C_P(0) = \sigma_P^2 \tag{3.6}$$

which are the mean square values of $f_1(t)$, $aM(t)$, $bN(t)$ and $P(t)$, respectively. Equation (3.6) shows that $C_M(\tau)$, $C_N(\tau)$ and $C_P(\tau)$ are all positive around $\tau = 0$ where their values add up in phase in equation (3.3).

Furthermore, both $N(t)$ and $P(t)$ have random properties and their autocovariance functions satisfy:

$$C_N(\infty) = 0;\ C_P(\infty) = 0 \tag{3.7}$$

This equation shows that both $N(t)$ and $P(t)$ become uncorrelated with themselves as time lag increases. Actually, $C_N(\tau)$ and $C_P(\tau)$ drop to a very low level as the time lag τ departs from zero.

In Equation (3.3), $C_{MNP}(\tau)$ represents the crosscorrelations among a deterministic and two random functions (all with zero mean). Unlike the autocovariance functions, $C_N(\tau)$ and $C_P(\tau)$, there will not be a particular time lag, τ, around which $C_{MNP}(\tau)$ can stand above the remaining components. This means that their components would usually be at low levels. In the case of a low SNR, this level is about the same as the components of $C_N(\tau)$ when the time lag, τ, is away from zero.

From the discussion above, it can be seen that the autocovariance function of $f_1(t)$ concentrates great amounts of energy of the second and fourth terms in Equation (2.10) around the zero time lag. So the two noise terms can be suppressed by editing the autocovariance function of $f_1(t)$ around the zero time lag. A simple way to edit the

autocovariance function is to Clip the Autocovariance Function of a Rectified Signal around the zero time lag (thus called the CAFRS technique).

4. ENVELOPE OF NARROWBAND NOISE

The main masking effects on $M(t)$ come from both $N(t)$ and $P(t)$. $N(t)$ is the envelope of narrowband noise, and $P(t)$ a function of $N(t)$ and $M(t)$ and of random character too. It is known that $M(t)$ is a real positive periodic function whose spectrum appears as a family of harmonics centred on zero frequency (in the case of one modulating source). But the probability property of $N(t)$ and its spectrum remain unknown and need to be further investigated in order to understand why editing the autocovariance function of a rectified vibration signal can enhance the signature, $M(t)$, of mechanical faults in rotating machines.

Both $N(t)$ and $\theta(t)$ in Equation (2.2) are random variables [5]. In the case of narrowband Gaussian noise, $\theta(t)$ is uniformly distributed in $[0, 2\pi]$ with a probability density function (PDF) of $0.5/\pi$, and for a fixed but arbitrary t, $N(t)$ obeys the Rayleigh probability law:

$$p[N(t)] = \frac{N(t)}{\alpha^2} e^{-N^2(t)/2\alpha^2} \tag{4.1}$$

as shown in Figure 4.1. For the Rayleigh distribution, its mean value is $\mu = \alpha\sqrt{\pi/2}$ and its variance $\sigma^2 = (2 - \pi/2)\alpha^2$.

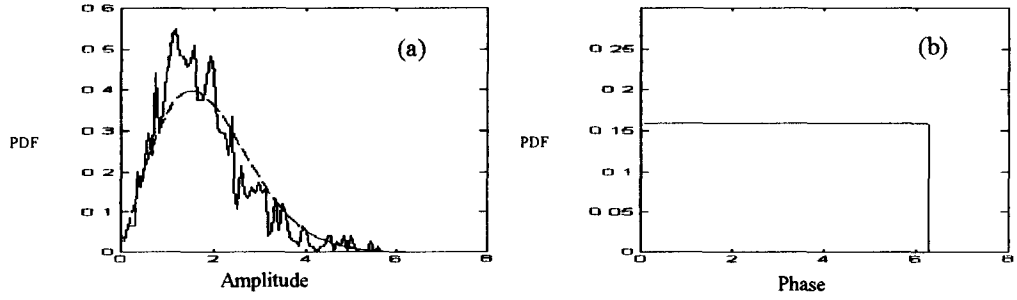

Figure 4.1. Probability Density Functions of (a) the Envelope [Dashed line - Generated Using Equation (4.1) and Solid Line - Obtained by Demodulating Equation (2.2) for a particular case] and (b) the Phase of the Narrowband Gaussian Noise.

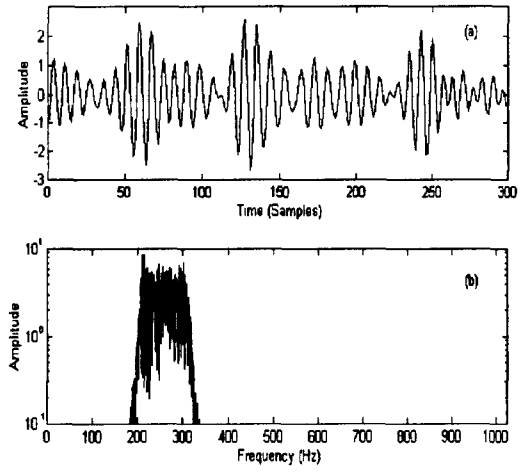

Figure 4.2. Narrowband Gaussian Noise: (a) Time Wave and (b) Spectrum.

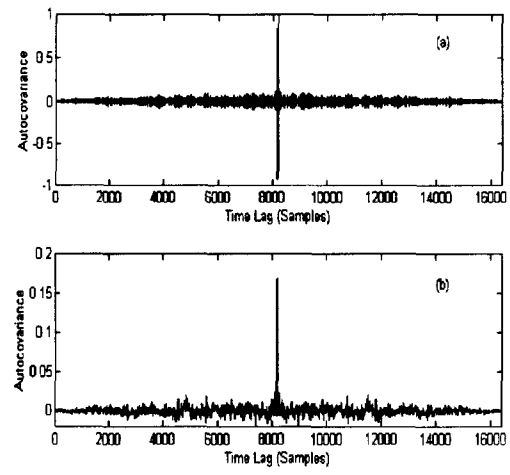

Figure 4.3. Autocovariance Functions of: (a) Narrowband Noise and (b) Its Envelope

This kind of noise can be generated by bandpass filtering a wideband noise with flat spectral density. Figure 4.2 shows an example of a narrowband noise generated in such a way. This figure clearly shows the modulating effects due to the slowly varying envelope, $N(t)$. Demodulating the narrowband noise by taking its absolute value and applying lowpass filtration produces the envelope, $N(t)$, which can be used to calculate its PDF. Figure 4.1 (a) shows a thus obtained PDF (solid line) which corresponds well to the theoretical one (dashed line).

Figure 4.3 compares the autocovariance function of the narrowband noise shown in Figure 4.2 with that of its envelope, $N(t)$. For both autocovariance functions, their components around $\tau = 0$ are well above (at least an order higher than) the remaining components. However, the prominent components in Figure 4.3 (a) vary between positive and negative while those in Figure 4.3 (b) are all positive.

5. APPLICATION

5.1. DIGITAL EXAMPLES

Digital sequences have been generated using Equation (2.4) to simulate a bearing with a outer race fault frequency of 16 Hz. This 'bearing fault' excites two resonances at 583 Hz and 677 Hz, respectively. The contamination of the bearing signal was composed of an additive frequency component of 37 Hz, and an additive noise signal centred on 600 Hz, with a bandwidth of 200 Hz.

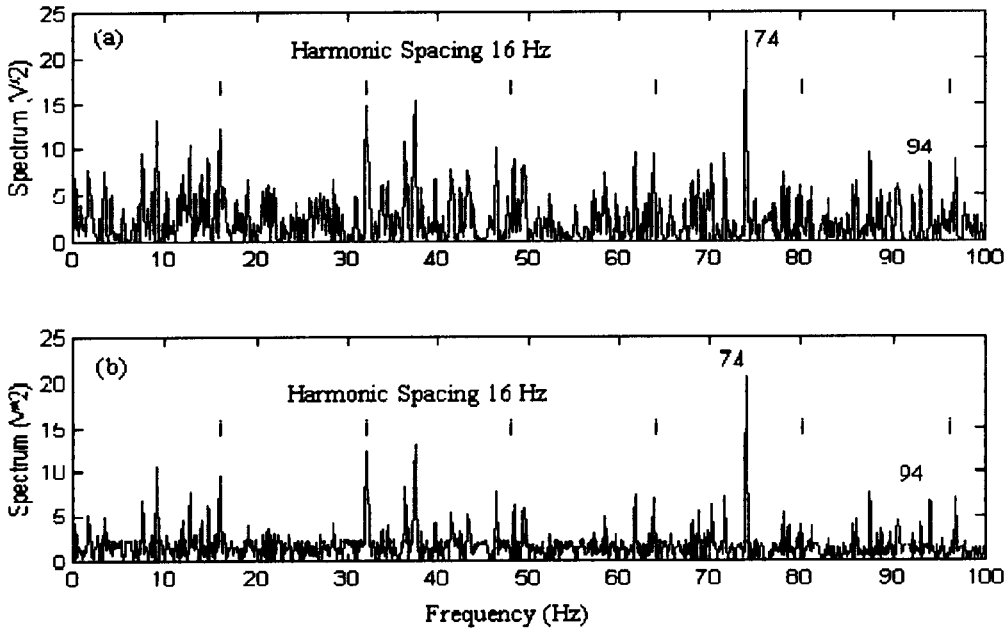

Figure 5.1. Spectra of Autocovariance Functions: (a) without Editing and (b) with Editing

Figure 5.1 shows the effect on the spectra of editing autocovariance functions for the case where the bearing signal and the discrete frequency component have the same RMS value, while the narrowband noise has triple this RMS value. The enhancement of the harmonic family of 16 Hz can be clearly envisaged by comparing Figure 5.1 (a) and (b). The discrete frequency component of 37 Hz is doubled to 74 Hz in Figure 5.1 and the frequency

component of 94 Hz is the difference frequency of the two carriers as predicted by Equation (2.6a).

5.2. MEASUREMENTS ON A RAILWAY TRACK

Analysed here is a composite bearing signal which was constructed using an array of seven accelerometers spaced at 1.8 m intervals along the track [6]. Track vibrations were caused by a passing train which had known bearing faults at known positions. The faulty bearing in question has two bad spalls on one of its cups (out-board race).

Figure 5.2 shows the spectra of the composite bearing signal. The two spectra were obtained using the BPFA and CAFRS procedures, respectively. Comparing Figure 5.2 (a) with Figure 5.2 (b) can help assess the ability of the CAFRS procedure to enhance the bearing signal in the case of low SNR. In Figure 5.2 (b), the peaks which stand out clearly at the bearing characteristic frequency of 61 Hz (its calculated value is 62.4 Hz at test speed 60 km/h) and up to its fourth harmonic (as marked by the cursors) give a good indication of a bad bearing with outer race defects.

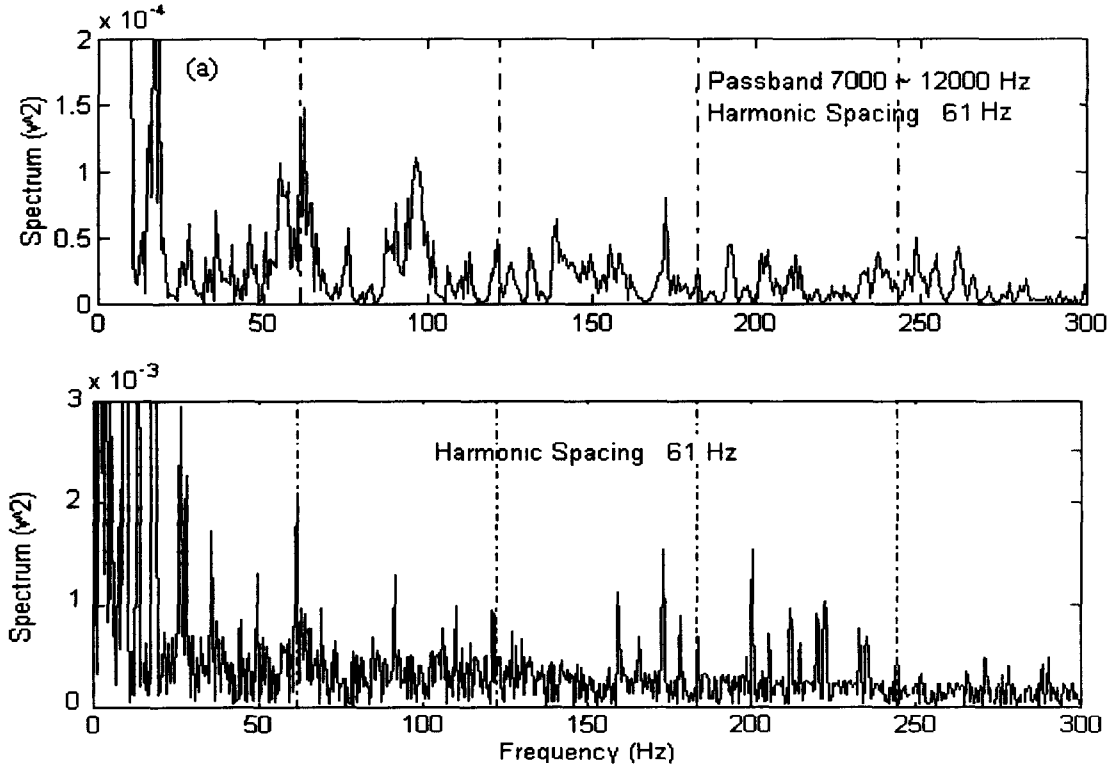

Figure 5.2. Spectra of the Composite Bearing Signal Obtained Using: (a) Bandpass Filtered Envelope Analysis and (b) the CAFRS Procedure.

5.3. MEASUREMENTS ON A PAPER MACHINE

The actual signal was measured on a paper machine with an outer race bearing fault [7]. Figure 5.3 shows the spectrum obtained using the CAFRS procedure. The harmonic family with a frequency spacing of 5.5 Hz is due to a pneumatic lubricator. The harmonic family (as marked by cursors) due to the bearing fault shows up clearly. It has been found that the bearing signal is mainly concentrated in the vicinity of 5.4 kHz [7]. This special case shows that the CAFRS procedure is able to reveal the bearing fault even when the bearing signal is concentrated within a single narrow frequency band, and even in the presence of considerable masking.

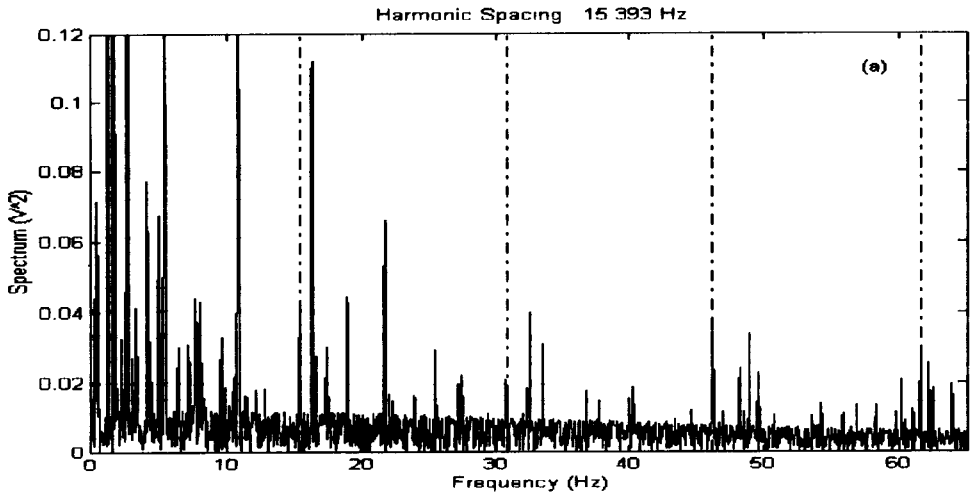

Figure 5.3. Spectrum obtained using: the CAFRS Procedure

6. CONCLUSIONS

In this paper, a new procedure is designed to diagnose bearing faults. This procedure is based on the Multiple Carrier Amplitude Demodulation (MCAD) technique and thus includes all the advantages of the MCAD technique. For many practical applications the MCAD technique can produce satisfactory results. However, the new procedure can produce still better results because of its ability to deal with a higher level of noise by enhancing the mechanical signatures contained in measured vibrations.

The new procedure is non-band dependent and is very useful in the case where it is difficult to find a frequency band in which bearing signals dominate. This is true for the practical application of detecting bearing faults from track response vibrations caused by passing trains, as studied in this paper.

References

[1]. S. Braun, "Mechanical Signature Analysis: Theory and Applications," Academic Press Inc. Ltd., London, UK, 1986.

[2]. P.D. McFadden and J. D. Smith, "Vibration Monitoring of Rolling Element Bearings by the High Frequency Resonance Technique --- a Review," Tribology International, 17(1), 1984, pp3-10.

[3]. Y. Gao, R, Ford and R. B. Randall, "Multiple Carrier Demodulation of Amplitude Modulations by Rectification: Application to the Detection of Mechanical Faults in Rotating Machines," Trans. I. E. Aust., Vol. ME21 No.s 3&4 137-145, 1996.

[4]. R.B. Randall, "Hilbert Transform Techniques in Machine Diagnosis," the International Conference on Rotordynamics, pp409-414, Tokyo, September, 1986.

[5]. H. Stark, *et al*, "Chapter 9, Modern Electrical Communications, Analog, Digital, and Optical Systems," 2nd Edition, Prentice Hall, Englewood Cliffs, NJ 07632, 1988.

[6] Gao, Y., Ford, R., and Randall, R.B., "Detection of Railway Bearing Faults by Enhancing Their Characteristic Properties Contained in Measured Track Response Vibrations," ARC Collaborative Research Project, Technical Report 8, 1996.

[7]. Randall, R. B. and Gao, Y., "Masking effects in digital envelope analysis of faulty bearing signals," I. Mech. E. Conference on Vibrations in Rotating Machines, pp351-359, Oxford, September, 1996.